J Nanostruct 13(2): 397-407, Spring 2023

RESEARCH PAPER

Silver-Chitosan Nanocomposite Prepared with Aqueous Sodium-Hydroxide and Aqueous Acetic Acid Solutions: Characteristics and Their Cytotoxic Effects

Laya Ebrahimi [1], Saeid Hosseinzadeh [1], Maryam Montaseri [1], Enayat Berizi [2], Mohammad Hashem Yousefi [1], Jaafar Jalaei [3], and Mansour Rahsepar [4]*

[1] *Department of Food Hygiene and Public Health, School of Veterinary Medicine, Shiraz University, Shiraz, Iran*

[2] *Nutrition Research Center, Department of Food Hygiene and Quality Control, School of Nutrition and Food Sciences, Shiraz University of Medical Sciences, Shiraz, Iran*

[3] *Department of Basic Sciences, School of Veterinary Medicine, Shiraz University, Shiraz, Iran*

[4] *Department of Materials Science and Engineering, School of Engineering, Shiraz University, Iran*

ARTICLE INFO

Article History:
Received 24 October 2022
Accepted 21 March 2023
Published 01 January 2023

Keywords:
Acetic acid
Cytotoxicity Nanoparticle
Silver-chitosan nanocomposite
Sodium-hydroxide

ABSTRACT

In this study, cytotoxic effects of silver-chitosan nanocomposites with aqueous sodium hydroxide solution (SCNC-ASHS) and aqueous acetic acid solution (SCNC-AAAS) were evaluated *in vitro*. The morphology of the synthesized nanoparticles was characterized by Fourier-Transform Infrared Spectroscopy (FTIR) and Scanning Electron Microscopy (SEM). Their cytotoxicities were then evaluated using MTT in concentrations of 1.56 to 400 µg/ml, and Acridine orange/Ethidium bromide (AO/EB) staining test after 24 h and 48 h. Results showed that the highest cytotoxicity was at 400 µg/ml concentration at which SCNC-ASHS respectively showed 80.57% and 84.37% toxicity on Vero and HT-29 cells after 24 h, and 82.20% and 84.84% after 48 h. While, the cytotoxicities for SCNC-AAAS on Vero and HT-29 cell lines were respectively 80.63% and 87.64% after 24 h, and 83.60% and 87.44% after 48 h. The most toxicity on HT-29 cells belonged to SCNC-AAAS with IC_{50} of 40.4 µg/ml. In the staining test, SCNC-AAAS revealed 41.84% HT-29 cell viability at 25 µg/ml concentration and 37.51% Vero cell viability at 6.25 µg/ml concentration. Generally, by increasing both SCNCs concentrations, the cell viabilities were decreased, and early and late apoptosis and necrosis were increased in AO/AE test. In conclusion, types of nanoparticles, synthesis methods, and different cell lines play considerable roles in inducing cytotoxicity. According to the higher significant cytotoxicity effects of both SCNCs on colon cancerous cells (HT-29) than normal cells (Vero) (p<0.05), it seems that they have anticancer effects; of those SCNC-AAAS displayed the higher effect with the IC_{50} of 4.4 µg/ml on HT-29 cells.

How to cite this article
Ebrahimi L., Hosseinzadeh S., Montaseri M., Berizi E. et al. Silver-Chitosan Nanocomposite Prepared with Aqueous Sodium-Hydroxide and Aqueous Acetic Acid Solutions: Characteristics and Their Cytotoxic Effects. J Nanostruct, 2023; 13(2):397-407. DOI: 10.22052/JNS.2023.02.010

* *Corresponding Author Email: hosseinzadeh@shirazu.ac.ir*

INTRODUCTION

Chitosan, a deacetylated derivative of chitin, is considered a food preservative due to its antimicrobial and antioxidant activities [1]. Chitosan has been applied in nanotechnology for packaging and coating due to its ability to form films [2]. The use of nanotechnology in the food industry is dramatically increasing due to the new properties of materials at the nanometer scale [3]. Nanoparticles are made of natural or synthetic polymers in a size range below 100 nm [4]. Chitosan nanoparticles, produced from the natural chitosan polymer, have displayed higher antimicrobial activity than chitosan [5]. In addition, chitosan nanocomposites can be used in developing drug delivery vectors and nanocomposites-based biosensors [6, 7]. Metal nanoparticles are also widely used in modern food coatings. Silver nanoparticles have been shown to possess antimicrobial properties because they degrade sulfur and phosphorus compounds in proteins and the genetic material of bacteria. The chitosan can be used as a matrix to place silver nanoparticles in coatings named silver-chitosan nanocomposites (SCNC) with antimicrobial properties [8-10]. Different chemical, physical, and biological techniques have been developed to synthetize SCNC [10-13]. Some studies have chemically prepared SCNC in an aqueous solution of acetic acid [10, 14] or aqueous sodium hydroxide [11, 15, 16].

The structures and sizes of SCNC can be characterized by Fourier transform infrared (FTIR) spectrophotometer, electron microscopy, UV spectrophotometer, X-ray powder diffraction (XRD), and surface-enhanced Raman spectroscopy (SERS) [10, 16, 17].

The toxicity of these nanoparticles, which are used as antimicrobial agents in food coatings, should be investigated because of their possibility of migration to foods and consumption by people. Various sizes of the nanoparticles and different types of cell lines affect their cytotoxicity. Accordingly, some reports showed the cytotoxicity, and anti-cancer effects of silver-chitosan nanocomposite on human umbilical artery endothelial cells (HUAECs) and A549 cells (Lung cancer cell line), respectively [18, 19]. In contrast, some publications advocated the non-toxicity of the chitosan-coated silver nanoparticles on healthy dermis cells (ATCC CRL-2522TM) and macrophages [8, 20, 21]. Furthermore, limited information is reported about different kinds and concentrations of the nanoparticles.

With respect to the various type of nanoparticles and the different types of cell lines, as well as limited information about the toxicity of the different types of nanoparticles and the nanoparticle concentrations, our study aimed to synthesize and investigate the toxicity of chitosan nanoparticles, and silver-chitosan nanocomposites, used in food coatings. Two synthesis methods of silver-chitosan nanocomposites (SCNC) were conducted, including aqueous acetic acid (SCNC-AAAS) and sodium hydroxide solutions (SCNC-ASHS), and the properties of the synthesized nanoparticles were investigated using various methods such as FTIR and SEM. The cytotoxic effects of these synthesized nanoparticles have not been assayed on Vero cells (the epithelial cell class of African green monkeys) as normal cells, and HT-29 cells (colon cancer cells), simultaneously that were studied in this research.

MATERIALS AND METHODS

Preparation of silver-chitosan nanocomposite (SCNC)

Preparation of SCNC with aqueous acetic acid solution (SCNC-AAAS)

SCNC-AAAS was synthesized according to the method of Honary et al. with the following modifications [14]. At first, 100 ml of chitosan solution (0.5 mg/ml) (Aldrich Chemical, Germany) was prepared in acetic acid solution (1-2%) (Merck, Germany). Due to the poor solubility, chitosan was kept at room temperature for 24 hours. Second, the prepared solution was added to 1 liter of 6 mM silver nitrate solution and was stirred for one hour on a stirrer (IKA, Germany). Third, the 58 mM sodium borohydride ($NaBH_4$) solution (Merck, Germany) was added dropwise until the color shifted from colorless to brown. Finally, the solution was heated at 50 °C in an oven (model CE.FH.151.4, Germany) to evaporate large amounts of water. The remained water was then completely removed by a freeze dryer (CHRIST, Germany).

Preparation of SCNC with aqueous sodium hydroxide solution (SCNC-ASHS)

SCNC-ASHS solution was synthesized according to Akmaz et al., as follows [11]. 100 mg of chitosan (Aldrich Chemical Company, Germany) was added

to 50 ml of 95 °C water. One ml of 0.02 M solution of silver nitrate ($AgNO_3$) (Merck, Germany) was added to the suspension during the sonication (Iranian Knowledge-Based Company of Nasir Research, Iran). Then, 100 µl of 0.3 M Sodium hydroxide (NaOH) solution (Merck, Germany) was added dropwise. At this stage, the color changed from colorless to reddish-yellow. The solution was sonicated for 10 minutes at 95 °C. The nanoparticles were then washed with distilled water and dried in an oven (Memmert, Germany) at 50 °C.

Examination of nanoparticle characteristic

Fourier-Transform Infrared Spectroscopy (FTIR)

FTIR method was used to determine the molecules and biological functional groups responsible for nanoparticle synthesis (NIRS XDS Process Analyzer, Metrohm) [22].

Scanning Electron Microscope (SEM)

SEM was applied to take images from the synthesized nanoparticles. The image details such as magnification and voltage were recorded in the related image (TESCAN, Czech Republic, model-TESCAN-Vega 3)

X-Ray Diffraction (XRD)

In the X-ray diffraction method, the SCNC-AAAS powder was placed on a glass slide and analysed using X-Ray diffractometer (Bruker D8 ADVANCE, Japan) which was set at photon energy of 40 KeV and 40 mA with CuKα1 beam with wavelength λ=1.54 at 2θ angle and angular range of 20 to 80 [23].

Cell culture

Two cell lines HT-29 and Vero were considered for the experiment. The cells initially freezed in cryotubes were transferred into sterile falcon tubes containing 10 ml of RPMI-1640 (for HT-29) or DMEM (for Vero) complete culture medium containing GlutaMax (Shell Max, Iran) supplemented with 10% fetal bovine serum (Gibco, USA), 1% penicillin-streptomycin (100 IU/ml and 100 µg/ml) (Bio-idea, Iran), and 0.05% amphotericin B (2.5 µg/ml) (Sigma, USA). The cells were then centrifuged (Biosan, Latvia) at 1000 rpm for 10 minutes, and the supernatants were discarded. The sediments containing 4×10^5 cells were then cultured in T-25 cell culture flasks containing the complete culture medium (6 ml) and incubated at 37 °C in 5% CO_2 and 95% humidity. The cell culture media were changed every 48 hours to achieve about 90% confluency [24]. The cells were then detached with 300 µl of 0.05% trypsin-versene solution (Bio-Idea Company, Iran) and were collected after the centrifugation (1000 rpm, 10 minutes) for the further cell treatment.

Cytotoxicity test

3-(4,5-dimethylthiazol-2-yl)-2,5-diphenyl-2H-tetrazolium bromide (MTT) test (Bio idea-Iran) was used to evaluate cell toxicity. Initially, 100 µl of culture medium containing 10^4 cells was added to each well of 96-well microplates to reach the appropriate cell confluency. The cells were then treated with SCNC-AAAS and SCNC-ASHS, and the cytotoxicity was fulfilled after 24h and 48h incubations. Both SCNCs were used at the concentrations of 400 µg/ml to 1.56 µg/ml with series of 2-fold dilutions. Afterwards, the wells were evacuated and washed with phosphate-buffered saline (PBS) (100 µl/well) three times. Three wells were considered for each concentration and the control group, receiving no treatment. MTT test was performed according to the instructions given by the manufacturer. Accordingly, 100 µl of RPMI-1640 without phenol red and 10 µl of MTT (12 mM) were added into 96-well plates containing cells and placed in a 37 °C incubator for 4 h. The wells contents were discarded and 50 µl of DMSO was added to each well. The plates were then incubated for 10 minutes at 37 °C. Finally, the microplates were measured at optical density (OD) value of 570 nm using a plate reader (BioTek, USA). This test was repeated three times, and the cytotoxicity percentage was calculated using the following equation [25, 26]:

$$\%\ \text{Cytotoxicity} = \left(1 - \frac{\text{OD of the sample}}{\text{OD of the control}}\right) \times 100$$

Acridine orange/Ethidium bromide (AO/EB) fluorescent staining

To evaluate cell apoptosis induced by SCNC-AAAS, AO/EB fluorescent staining was applied for both HT-29 and Vero cells. Firstly, 1×10^5 cells/well were seeded into 12-well tissue culture plates. After 72h incubation, the supernatants were discarded, and the monolayer cells were washed with PBS and supplemented with 6.25 µg/ml, 12.5 µg/ml, and 25 µg/ml SCNC-AAAS for HT-29 cell line,

and 1.56 µg/ml, 3.12 µg/ml, and 6.25 µg/ml SCNC-AAAS for Vero cells. Negative controls, without any treatment, were considered for both cell lines. The cells were incubated for 24h (37 ºC, 5% CO_2) and then harvested using 200 µl of EDTA (1 mM). After adding 2 ml RPMI-1640 or DMED medium supplemented with 10% FBS, the cells were centrifuged, and 200 µl medium was added to the remained cells. 20 µl of the cell suspension was mixed with an ethidium bromide/acridine orange dye. Then, 10 µl of the dyed cells was transferred to a hemocytometer slide and assessed using a fluorescence microscope (CETI, 040856, Belgium) at ×20 magnification [24, 27].

Preparation of cells for microscopy

Preparation of cells for the phase-contrast microscopy

About 1.5×10^5 cells (HT-29 or Vero cells), suspended in 2 ml of RPMI-1640 or DMEM medium, were seeded into six-well plates and incubated (37°C, 5% CO_2). After the cell monolayer formation, 400 µg/ml of each SCNCs-AAAS and SCNCs-ASHS were added to both HT-29 and Vero cell lines, and the plates were incubated (37°C, 5% CO_2) for 24h. The cells were examined by phase-contrast microscopy (Optika, Italy) at ×10 magnification morphologically [28].

Preparation of cells for the scanning electron microscopy (SEM)

About 1.5×10^5 cells (HT-29 or Vero cells) in 2 ml of the media were initially cultured in six-well plates and incubated. After the formation of the cell monolayers, the cells were evaluated by adding different concentrations of SCNC-AAAS or SCNC-ASHS into the wells and were incubated for 24 hours. SCNC-AAAS concentrations were considered to be 100 µg/ml in Vero cells and 12.5 µg/ml in HT-29 cells, while SCNC-ASHS was added at a concentration of 100 µg/ml and 6.25 µg/ml in HT-29 cells and Vero cells, respectively. The cells were then washed with PBS (2 ml/well) and fixed with 3% glutaraldehyde (2 ml/well) (Dae Jung, Korea) for 2 hours at 4° C. To dehydrate the cells, alcohol solutions (2 ml/well) (Merck, Germany) with concentrations of 50%, 60%, 70%, 80%, 90%, and 100% were exerted for 30 minutes for each concentration. The plates were finally kept in a laminar flow hood for 2h at room temperature. The cell images were then taken by scanning electron microscopy [29].

Statistical analysis

All data were analyzed as mean ± standard deviation (SD) in triplicate experiment. Statistical significance for MTT test was determined by one-way analysis of variance and independent t-test using SPSS v.19 software. $P < 0.05$ was considered statistically significant. IC_{50} was calculated using the non-linear regression analysis method in GraphPad Prism v.8.3.0 software.

RESULTS AND DISCUSSION

SCNCs Microscopy

FTIR spectroscopy

Fourier transform infrared spectroscopy analysis was carried out to identify the chemical structures of SCNC-AAAS and SCNC-ASHS. Details are given in Fig. 1. The spectral shifts of the diagram in the 3350 cm^{-1} frequency show the presence of amine and hydroxyl groups and their overlap. Also, the shifts that occurred in the 2880 cm^{-1} wavenumber resulted from the presence of CH_2 in chitosan and nanocomposite. The peak observed at 1513 cm^{-1} indicates the bending vibration of the NH band. It is noticeable that the interaction of NH_2 or O-H groups of chitosan with silver ions tends their vibrations peak to lower wavenumbers. The sharp peak observed in the 1284 cm^{-1} wavenumber represents the CH_2 wagging vibrations. The changes in the frequency range from 1060 to1020 cm^{-1} usually correspond to C-N and C-O stretching vibrations in which the C-O stretching vibrations are formed in the frequency of the composite combined. The relatively sharp peak detected in the frequency of 800 cm^{-1} indicates the absorption of NO_3^- ions from silver nitrate salt. The peak observed in 670 cm^{-1} can result from reducing the activity of chitosan and metallic silver precipitation. Seemingly, the saccharide structure changes after adsorption of silver ions detectable at 1050 cm^{-1} peak [23, 30].

Scanning Electron Microscopy

The size and morphology of the nanocomposites recorded by SEM are shown in Fig. 2. SCNC-AAAS are detectable with cubic shapes and with both sizes of smaller and larger than 100 nm; while SCNC-ASAH are spherical-shape with a size smaller than 100 nm.

X-Ray Diffraction (XRD)

To detect nanoparticle composition we used other techniques including X-Ray powder

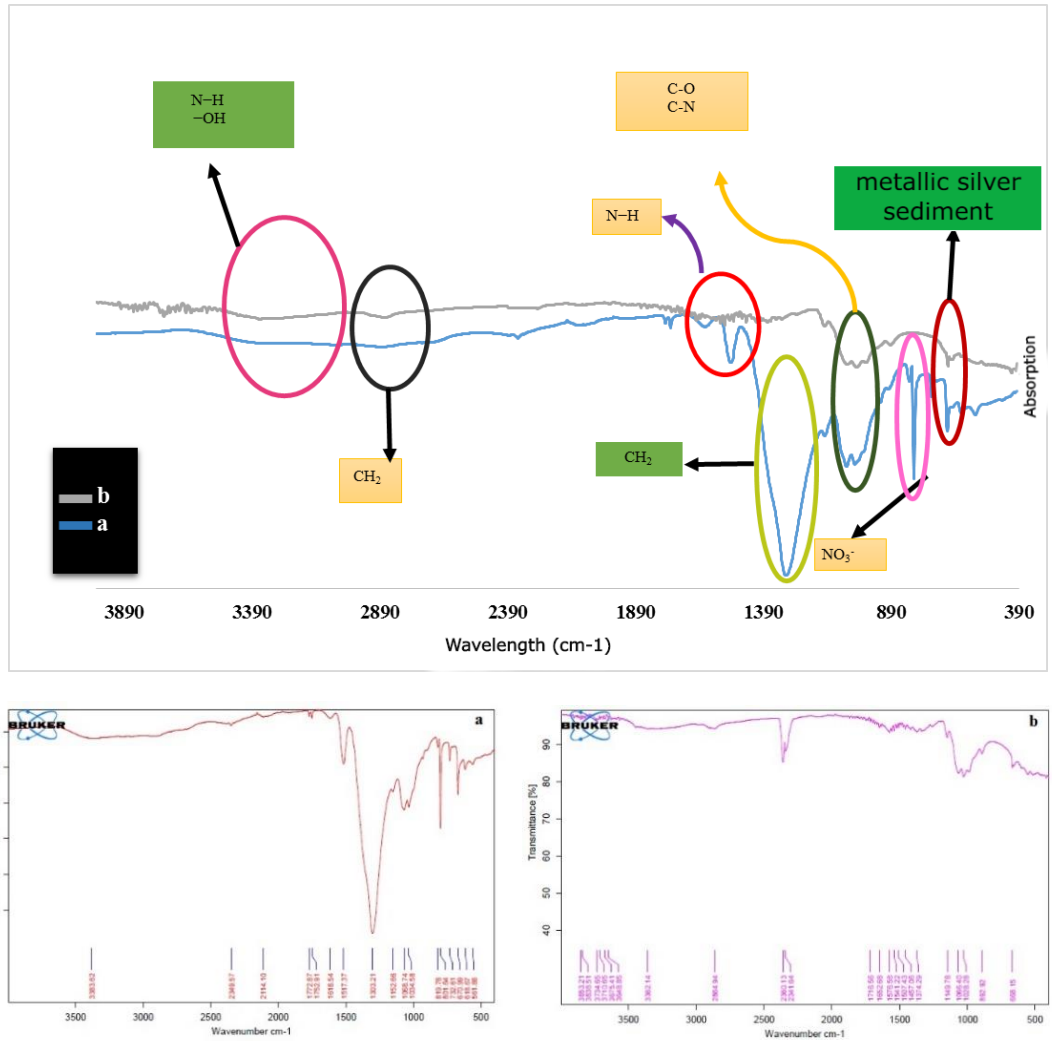

Fig. 1. Fourier transform infrared (FTIR) spectroscopy analysis to identify the chemical structures of SCNC-AAAS and SCNC-ASHS. (a) The characterized peak of silver chitosan nanocomposite with aqueous acetic acid solution (SCNCs-AAAS), (b) the characterized peak of silver chitosan nanocomposite with aqueous sodium hydroxide solution (SCNCs-ASHS).

Diffraction (XRD) according to previous studies. According to the higher cytotoxicity effect of SCNC-AAAS, XRD was only used for this nanocomposite chitosan. Fig. 3 shows the pattern of silver chitosan nanocomposites with aqueous acetic acid solution. The peaks at the angles of 38.23, 44.44, 64.54 and 77.62 degrees are assigned to silver at 111, 200, 220, and 311 diffusers, respectively. The broad peak at 22.5 degrees is related to the presence of chitosan.

Cytotoxicity

The cytotoxicity effects of SCNC-ASAH (from 400 to 1.56 µg/ml) on HT-29 and Vero cells are shown in Fig. 4. The cytotoxicity of SCNC-ASAH on HT-29 and Vero cells was significantly increased between the time 24h and 48h, and the nanoparticle concentrations (p<0.05)

IC_{50} value of SCNCs in HT-29 and Vero cell lines

The IC_{50} values of SCNC-AAAS in HT-29 and Vero cells were determined as 4.4 and 13.40 µg/ml, respectively. Since HT-29 cell line showed a lower IC_{50} value, its toxicity to SCNC-AAAS was higher than that of Vero cells. Furthermore, IC_{50} values of SCNC-ASHS in HT-29 and Vero cells were calculated

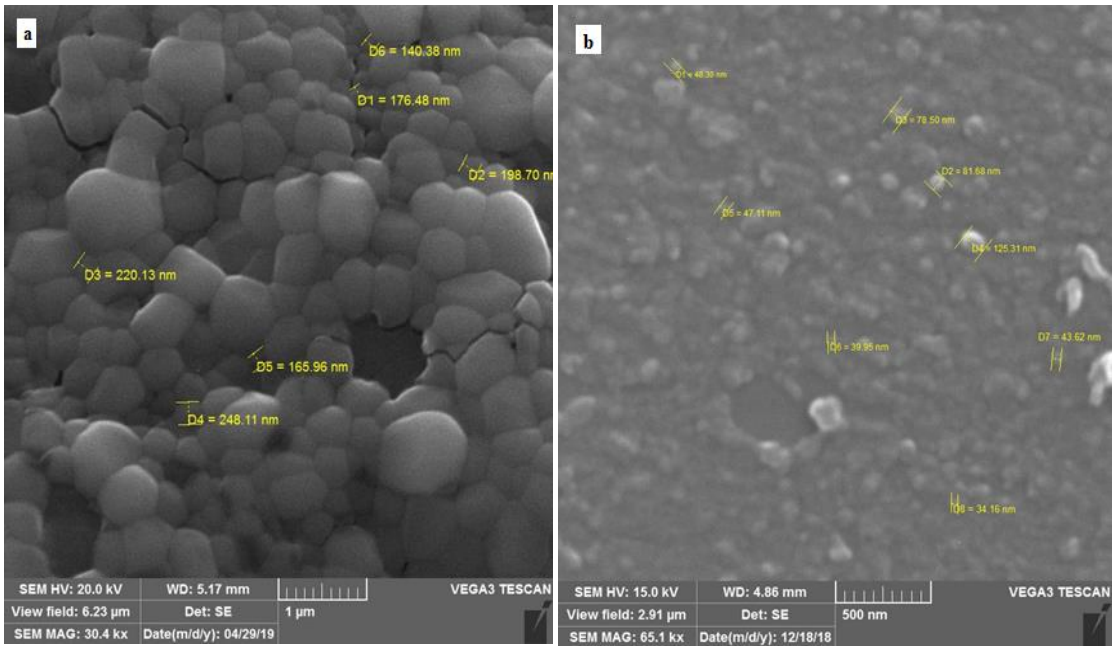

Fig. 2. Scanning Electron Microscopy (SEM) images to characterize the size and morphology of the nanocomposites. (a) Silver chitosan nanocomposite with aqueous acetic acid solution (SCNCs-AAAS) are cubic shapes and the sizes of smaller and larger than 100 nm, and (b) silver chitosan nanocomposite with aqueous sodium-hydroxide (SCNCs-ASHS) solution are spherical-shape and smaller than 100 nm.

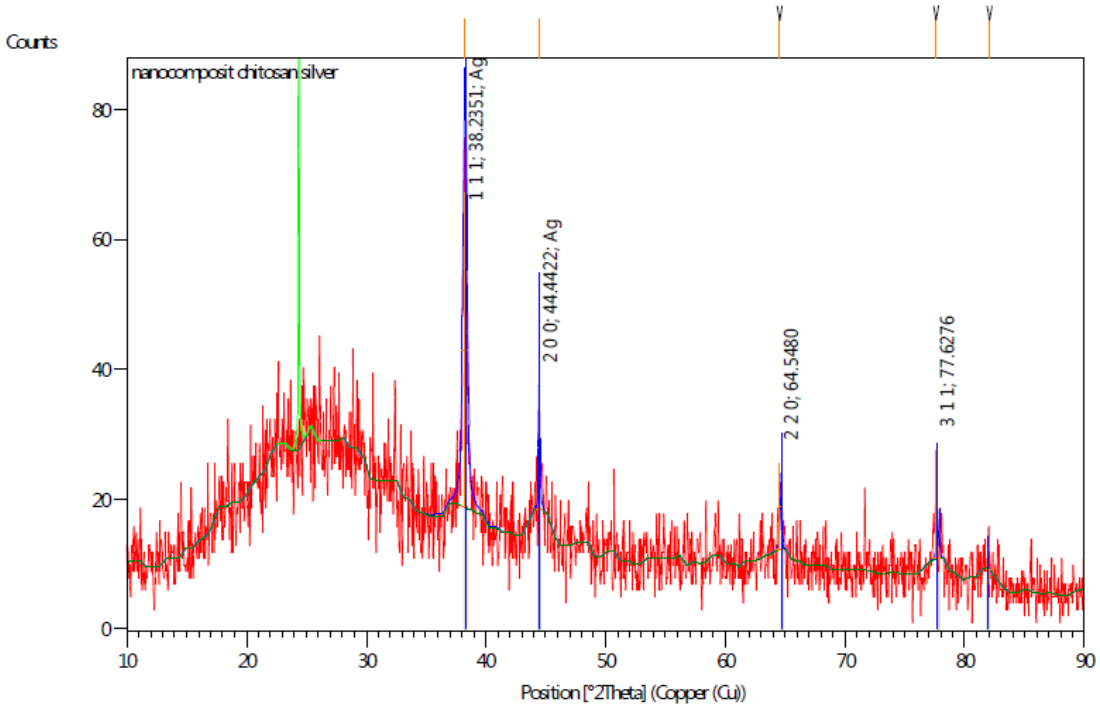

Fig. 3. X-Ray Diffraction (XRD) result for SCNC-AAAS. The peaks at the angles of 38.23, 44.44, 64.54 and 77.62 degrees are assigned to silver at 111, 200, 220, and 311 diffusers, respectively. The broad peak at 22.5 degrees belongs to chitosan.

at 11.54 and 19.36 µg/ml, respectively. The lower IC_{50} value of HT-29 cells implied higher cell toxicity to SCNC-ASHS than that of Vero cells.

Acridine orange/Ethidium bromide (AO/EB) fluorescent staining

The cell viability, early apoptosis, late apoptosis, and necrosis were examined in the presence of SCNC-AAAS and SCNC-ASHS by AO/EB staining (Fig. 5). The results showed that when SCNCs concentrations increased, cell viability rates decreased, and early apoptosis, late apoptosis, and necrosis increased.

Cell microscopy treated with different concentrations of SCNCs

Phase-contrast microscopy

Changes in morphology of both HT-29 and Vero

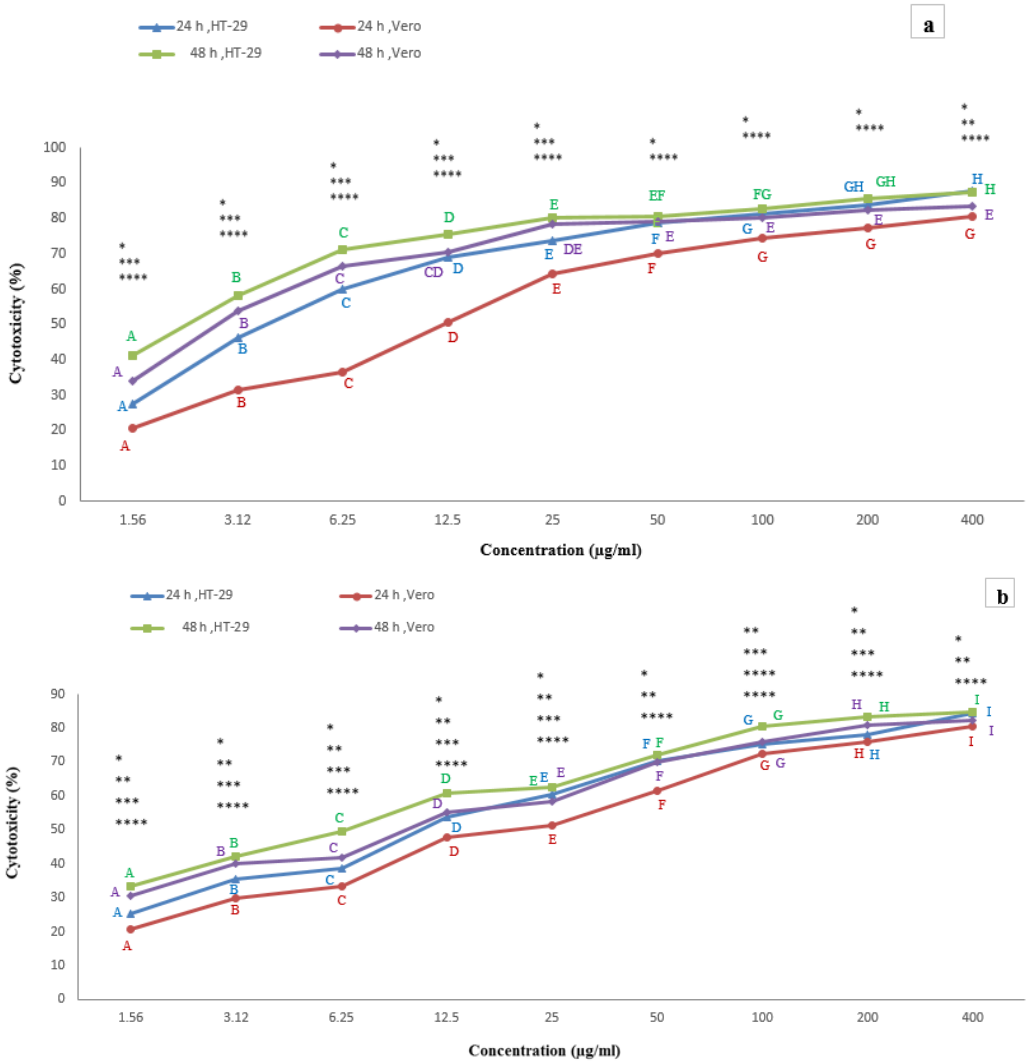

Fig. 4. The cytotoxic effects of the nanocomposites on HT-29 and Vero cells. (a) Various concentrations (1.56 µg/ml to 400 µg/ml) of silver chitosan nanocomposite with aqueous acetic acid solution (SCNC-AAAS), and (b) silver chitosan nanocomposite with aqueous sodium-hydroxide solution (SCNC-ASHS) after 24 h and 48 h.

Similar letters denote no statistically significant difference between different concentrations. The sign * represents a significant difference in 24 hours between HT-29 and Vero cells, the sign ** represents a significant difference in 48 hours between HT-29 and Vero cells, the sign *** represents a significant difference between the two times of 24 and 48 hours in HT-29 cells, and the sign **** represents a significant difference between the two times of 24 and 48 hours in the Vero cell ($p < 0.05$).

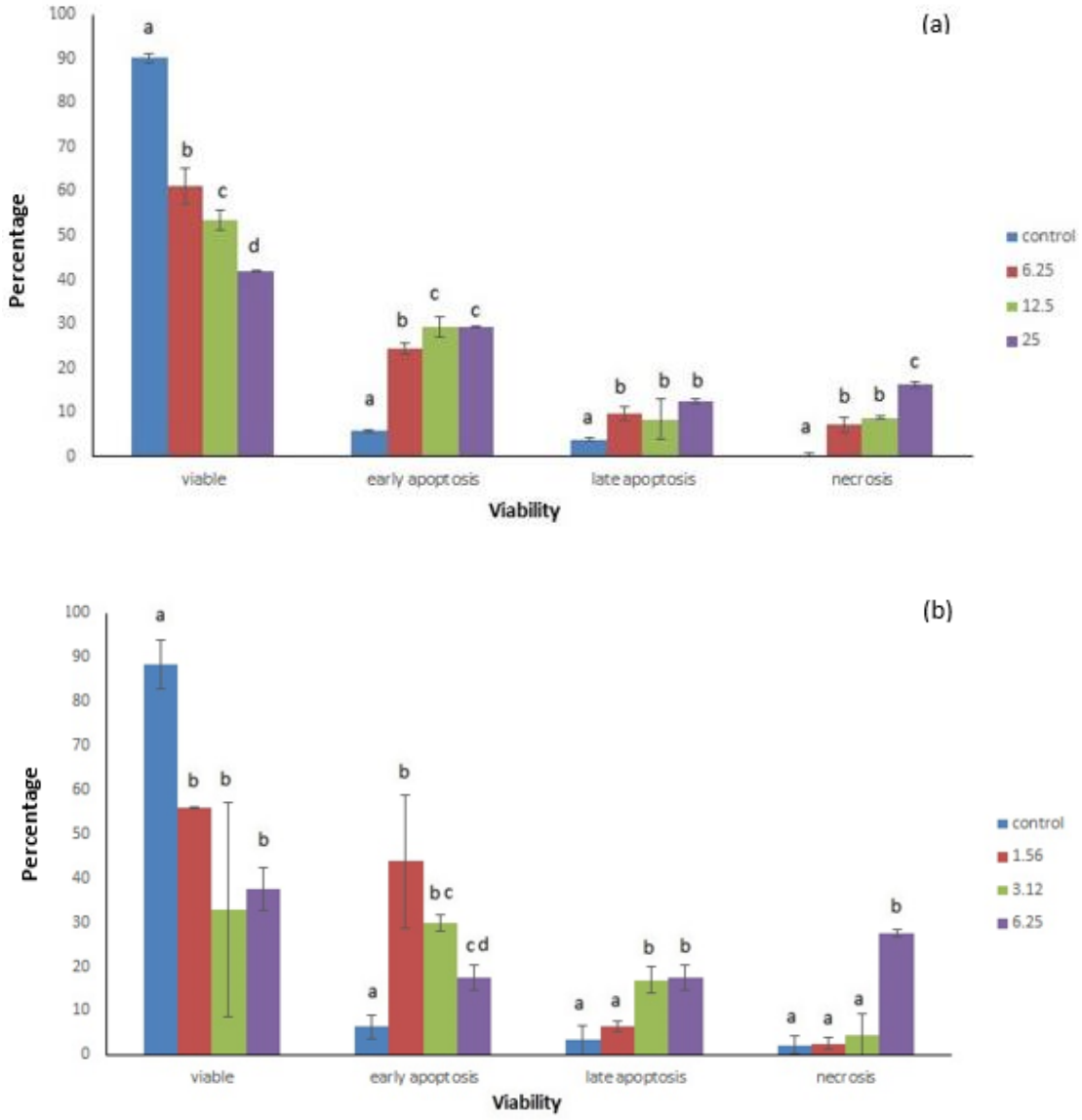

Fig. 5. Viability, early apoptosis, late apoptosis, and necrosis of HT-29 cells (a) and Vero cells (b) in the presence of various concentrations of silver chitosan nanocomposite with aqueous acetic acid solution (SCNC-AAAS) after 72 h using acridine orange/ethidium bromide (AO/EB) fluorescent staining.
Similar letters denote no statistically significant difference between different concentrations ($p>0.05$)

cells after 24 hours of treatment with SCNC-AAAS and SCNC-ASHS nanoparticles were recorded by contrast phase microscopy. Changes such as decreased cell adhesion and increased floating cells were observed.

Scanning Electron Microscopy

The cell morphology changes after 24h of treatment are illustrated in Fig. 6. The control group, which did not receive any treatments, showed a normal shape and surface, while the treated cells were changed to a honeycomb structure, and holes appeared in the cell membrane. Cell death resulted from leakage of intracellular contents throughout the cell membrane.

The antimicrobial properties of chitosan have been enhanced by loading chitosan with various metals. Among all antimicrobial metals, silver

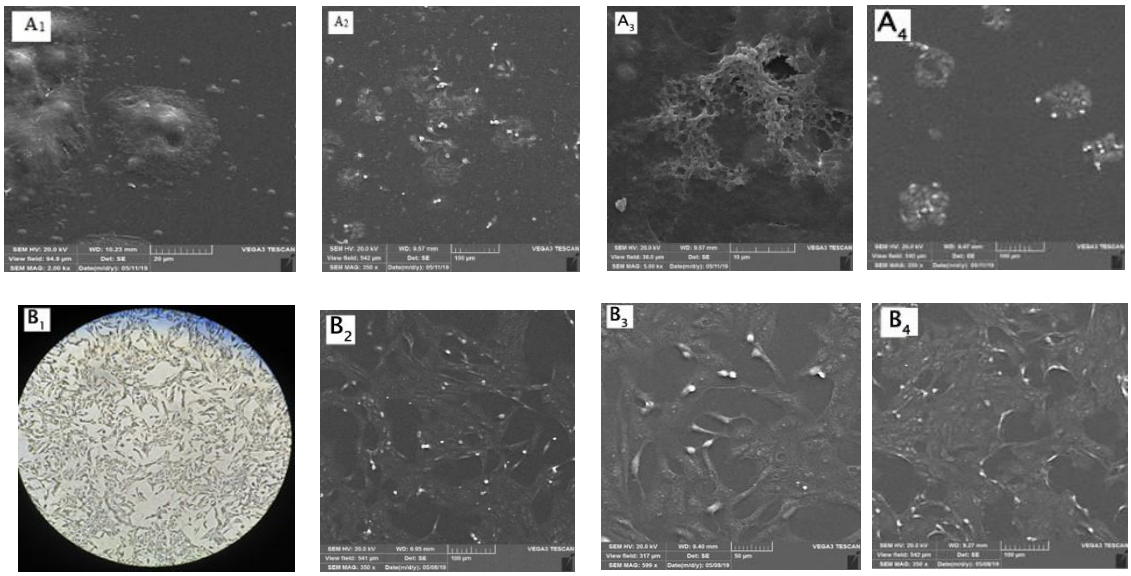

Fig. 6. Effects of silver chitosan nanocomposite with aqueous acetic acid solution (SCNCs-AAAS) (A2, B2), and silver chitosan nanocomposite with aqueous sodium-hydroxide solution (SCNCs-ASHS) (A3, B3) on morphology of Vero and HT-29 cells.
A: HT-29 cell line, and B: Vero cell line. A1: control group (concentration of 0 µg/ml), A2, A3 and A4: concentration of 400 µg/ml; and B1: the fixed cells shown by contrast phase microscope at 10x magnification before scanning electron microscopy image, B2: control group (concentration of 0 µg/ml), B3: concentration of 12.5 µg/ml, and B4: concentration of 6.25 µg/ml.

possesses great toxicity against a wide range of microorganisms. Nanocomposites based on silver nanoparticles (SNPs) have been used as antimicrobial films for food packaging [30]. However, the toxicology of SNPs has remained unknown. Additionally, SNPs can be absorbed into the bloodstream via different routes of administration, leading to the deposition of silver in many organs, including the liver and spleen, and potentially can damage the organ. Previous studies have shown that different surface stabilizers have distinct impacts on SNPs cytotoxicity. Because of its good biocompatibility and antibacterial properties, chitosan is often employed as the active ingredient of topical wound materials in combination with SNPs [31]. Chitosan is also used as a stabilizer instead of a chemical reducing agent for protecting SNPs from agglomeration [11].

In the present study, chitosan was employed for producing SCNC in which sodium borohydride and sodium hydroxide were used as reducing agents for silver ions to produce SCNC-AAAS and SCNC-ASHS, respectively. They revealed cytotoxic effects on both HT-29 colon cancer cells and normal Vero cells, depending to the dose and time. Palem et al. reported a 5-7% cytotoxicity on normal 3T3 fibroblasts and cancer Hela cells in the presence of SCNC [32]. Their results were in accordance with our findings. In the present study, toxicity was observed on both normal (Vero) and cancer (HT-29) cells in the presence of both SCNCs. However, SCNC-AAAS showed more toxicity towards HT-29 cells with the IC_{50} of 4.4 µg/ml, representing the possibility of its anti-cancer effect. Another study found that chitosan/silver nonocomposite had cytotoxicity toward breast cancer (MCF-7) cell, however chitosan/silver/multiwalled carbon nanotubes showed higher effect [14]. SCNC is reported to have an anti-cancer effect on A549 lung cancer cells, with IC_{50} of 29.35 µg/ml [18]. This study also showed that SCNC-AAAS and SCNC-ASHS with IC_{50} of 4.40 and 11.54 µg/ml possessed anti-cancer effects on HT-29 cells, respectively. It is indicated that Ag-doped chitosan-poly vinyl alcohol nanocomposites impact more on human liver cancer (HEPG2) cells with IC_{50} of 43.7 µg/ml than breast cancer (MCF7) cells with IC_{50} of 52.5 µg/ml [33]. This result is in accordance with our findings.

Tyliszczak et al. stated that chitosan-based hydrogels modified with SNPs produced by sodium borohydride in concentrations of 25, 50, 75, and 100 (wt%) showed no toxic effect on dermis cells BJ (CRL-2522TM) [8]. Wang et al. reported that

silver immobilized in the sliver nanoparticle-doped chitosan composite films shows a significant influence on the cell adhesion and subsequent proliferation of human umbilical vein endothelial cells [19]. Jena et al. reported that chitosan-coated silver nanoparticles, using chitosan as stabilizing and reducing agent, showed no significant cytotoxic or DNA damage on the macrophages at the bactericidal dose [21]. The less toxic effects of SCNCs in former studies were likely due to the type of cells. A reason for the non-toxicity of SCNC in the mentioned studies compared to the present study is the difference in the type of investigated cells so that normal dermis cells, umbilical vein endothelial cells, and macrophages exerted more resistance to SCNCs compared to normal kidney epithelial cells. SCNC size is another reason. SCNC size is a considerable aspect of different results, which can be varied from less than 10 nm to more than 100 nm, in our study. It seems that larger size (100 nm) of SCNCs causes more cell biological disorders in comparison with smaller particles (10 nm) [8, 34]. Another influential factor is the methods SCNC synthesis. In the current study, chitosan was alternatively used as a silver ion reducing agent instead of sodium borohydride, used in previous studies. Jena et al. showed that the same-size particles above 100 nm were not toxic to the macrophage [21]. Because of the cytotoxicity of our nanoparticles on the normal cells, their application is not recommended in food coatings. Our synthetized nanoparticles were highly toxic on the cancerous cells, and more investigations are recommended to survey their appropriate effects on treating cancers.

CONCLUSION

In the present study, SCNC-AAAS and SCNC-ASHS showed more toxic effects on the cancerous cells than the normal cells. However, SCNC-AAAS showed a higher toxic effect on both normal and cancer cell lines compared to SCNC-ASHS. The results implied that the synthesis procedure of SCNCs plays a notable role in the cytotoxicity of the nanoparticles. Because of their highly toxic effects on the normal cell line, both types of SCNCs, are not recommended for the food industry. Nevertheless, due to their probable anti-cancer effects, found in cell culture assay, they may be applicable in the treatment of colon cancer which requires more subsequent studies. Furthermore, according to the results, exposure time, the nanoparticles concentrations, the procedure of nanoparticle synthesis, and the cell line types considerably can affect SCNCs cytotoxicities.

ACKNOWLEDGMENTS

The authors gratefully acknowledge the Research Affair of Shiraz University.

CONFLICT OF INTEREST

The authors declare that there is no conflict of interests regarding the publication of this manuscript.

REFERENCES

1. Pourmahdi Borujeni M, Keshavarz Z. Effect of chitosan and nanochitosan on reducing acid tolerance of Listeria monocytogenes. Iran J Vet. 2015 1;11(3):56-66.
2. Sabaghi M, Maghsoudlou Y, Khomeiri M, Ziaiifar AM. Active edible coating from chitosan incorporating green tea extract as an antioxidant and antifungal on fresh walnut kernel. Postharvest Biol Technol. 2015;110:224-228.
3. Narayanan KB, Sakthivel N. Green synthesis of biogenic metal nanoparticles by terrestrial and aquatic phototrophic and heterotrophic eukaryotes and biocompatible agents. Adv Colloid Interface Sci. 2011;169(2):59-79.
4. Gao W, Lai JCK, Leung SW. Functional enhancement of chitosan and nanoparticles in cell culture, tissue engineering, and pharmaceutical applications. Front Physiol. 2012;3.
5. Zarei M, Ramezani Z, Ein-Tavasoly S, Chadorbaf M. Coating Effects of Orange and Pomegranate Peel Extracts Combined with Chitosan Nanoparticles on the Quality of Refrigerated Silver Carp Fillets. J Food Process Preserv. 2015;39(6):2180-2187.
6. Jiang Y, Wu J. Recent development in chitosan nanocomposites for surface-based biosensor applications. Electrophoresis. 2019;40(16-17):2084-2097.
7. Motiei M, Kashanian S, Taherpour A. Hydrophobic amino acids grafted onto chitosan: a novel amphiphilic chitosan nanocarrier for hydrophobic drugs. Drug Dev Ind Pharm. 2016;43(1):1-11.
8. Tyliszczak B, Drabczyk A, Kudłacik-Kramarczyk S, Bialik-Wąs K, Kijkowska R, Sobczak-Kupiec A. Preparation and cytotoxicity of chitosan-based hydrogels modified with silver nanoparticles. Colloids Surf B Biointerfaces. 2017;160:325-330.
9. Karthik CS, Chethana MH, Manukumar HM, Ananda AP, Sandeep S, Nagashree S, et al. Synthesis and characterization of chitosan silver nanoparticle decorated with benzodioxane coupled piperazine as an effective anti-biofilm agent against MRSA: A validation of molecular docking and dynamics. Int J Biol Macromol. 2021;181:540-551.
10. Nandana CN, Christeena M, Bharathi D. Synthesis and Characterization of Chitosan/Silver Nanocomposite Using Rutin for Antibacterial, Antioxidant and Photocatalytic Applications. J Cluster Sci. 2021;33(1):269-279.
11. Akmaz S, Dilaver Adıgüzel E, Yasar M, Erguven O. The Effect of Ag Content of the Chitosan-Silver Nanoparticle

Composite Material on the Structure and Antibacterial Activity. Adv Mater Sci Eng. 2013;2013:1-6.
12. Shah A, Hussain I, Murtaza G. Chemical synthesis and characterization of chitosan/silver nanocomposites films and their potential antibacterial activity. Int J Biol Macromol. 2018;116:520-529.
13. Abdel-Aziz MM, Elella MHA, Mohamed RR. Green synthesis of quaternized chitosan/silver nanocomposites for targeting mycobacterium tuberculosis and lung carcinoma cells (A-549). Int J Biol Macromol. 2020;142:244-253.
14. Honary S, Ghajar K, Khazaeli P, Shalchian P. Preparation, Characterization and Antibacterial Properties of Silver-Chitosan Nanocomposites Using Different Molecular Weight Grades of Chitosan. Trop J Pharm Res. 2011;10(1).
15. Murugadoss A, Chattopadhyay A. A 'green' chitosan–silver nanoparticle composite as a heterogeneous as well as micro-heterogeneous catalyst. Nanotechnology. 2007;19(1):015603.
16. Freitas DS, Teixeira P, Pinheiro IB, Castanheira EMS, Coutinho PJG, Alves MJ. Chitosan Nano/Microformulations for Antimicrobial Protection of Leather with a Potential Impact in Tanning Industry. Materials. 2022;15(5):1750.
17. Kang Y, Kim HJ, Lee SH, Noh H. Paper-Based Substrate for a Surface-Enhanced Raman Spectroscopy Biosensing Platform—A Silver/Chitosan Nanocomposite Approach. Biosensors. 2022;12(5):266.
18. Arjunan N, Kumari HLJ, Singaravelu CM, Kandasamy R, Kandasamy J. Physicochemical investigations of biogenic chitosan-silver nanocomposite as antimicrobial and anticancer agent. Int J Biol Macromol. 2016;92:77-87.
19. Wang X-h, Wang Z, Zhang J, Qi H-x, Chen J, Xu M. Cytotoxicity of AgNPs/CS composite films: AgNPs immobilized in chitosan matrix contributes a higher inhibition rate to cell proliferation. Bioengineered. 2016;7(5):283-290.
20. Hernández-Sierra JF, Galicia-Cruz O, Salinas-Acosta A, Ruíz F, Pierdant-Pérez M, Pozos-Guillén A. In vitro Cytotoxicity of Silver Nanoparticles on Human Periodontal Fibroblasts. J Clin Pediatr Dent. 2011;36(1):37-42.
21. Sonawnae A, Jena, Mohanty, Mallick, Jacob. Toxicity and antibacterial assessment of chitosan-coated silver nanoparticles on human pathogens and macrophage cells. Int J Nanomed. 2012:1805.
22. Loutfy SA, Alam El-Din HM, Elberry MH, Allam NG, Hasanin MTM, Abdellah AM. Synthesis, characterization and cytotoxic evaluation of chitosan nanoparticles:in vitro liver cancer model. Advances in Natural Sciences: Nanosci Nanotechnol. 2016;7(3):035008.
23. Kumar-Krishnan S, Prokhorov E, Hernández-Iturriaga M, Mota-Morales JD, Vázquez-Lepe M, Kovalenko Y, et al. Chitosan/silver nanocomposites: Synergistic antibacterial action of silver nanoparticles and silver ions. Eur Polym J. 2015;67:242-251.
24. Kawarizadeh A, Pourmontaseri M, Farzaneh M, Hossinzadeh S, Pourmontaseri Z. Cytotoxicity, apoptosis, and IL-8 gene expression induced by some foodborne pathogens in presence of Bacillus coagulans in HT-29 cells. Microb Pathog. 2021;150:104685.
25. Kawarizadeh A, Pourmontaseri M, Farzaneh M, Hosseinzadeh S, Ghaemi M, Tabatabaei M, et al. Interleukin-8 gene expression and apoptosis induced by Salmonella Typhimurium in the presence of Bacillus probiotics in the epithelial cell. J Appl Microbiol. 2020;131(1):449-459.
26. Poormontaseri M, Hosseinzadeh S, Shekarforoush SS, Kalantari T. The effects of probiotic Bacillus subtilis on the cytotoxicity of Clostridium perfringens type a in Caco-2 cell culture. BMC Microbiol. 2017;17(1).
27. Hosseinzadeh N, Shomali T, Hosseinzadeh S, Raouf Fard F, Pourmontaseri M, Fazeli M. Green synthesis of gold nanoparticles by using Ferula persica Willd. gum essential oil: production, characterization and in vitro anti-cancer effects. J Pharm Pharmacol. 2020;72(8):1013-1025.
28. Lee Y-H, Cheng F-Y, Chiu H-W, Tsai J-C, Fang C-Y, Chen C-W, et al. Cytotoxicity, oxidative stress, apoptosis and the autophagic effects of silver nanoparticles in mouse embryonic fibroblasts. Biomaterials. 2014;35(16):4706-4715.
29. Saudi A, Rafienia M, Zargar Kharazi A, Salehi H, Zarrabi A, Karevan M. Design and fabrication of poly (glycerol sebacate)-based fibers for neural tissue engineering: Synthesis, electrospinning, and characterization. Polym Adv Technol. 2019;30(6):1427-1440.
30. Kaur P, Thakur R, Barnela M, Chopra M, Manuja A, Chaudhury A. Synthesis, characterization and in vitro evaluation of cytotoxicity and antimicrobial activity of chitosan-metal nanocomposites. J Chem Technol Biotechnol. 2014;90(5):867-873.
31. Peng Y, Song C, Yang C, Guo Q, Yao M. Low molecular weight chitosan-coated silver nanoparticles are effective for the treatment of MRSA-infected wounds. Int J Nanomed. 2017;Volume 12:295-304.
32. Palem RR, Saha N, Shimoga GD, Kronekova Z, Sláviková M, Saha P. Chitosan–silver nanocomposites: New functional biomaterial for health-care applications. Int J Polym Mater Polym Biomater. 2017;67(1):1-10.
33. Abaza A, Mahmoud GA, Hegazy EA, Amin M, Shoukry E, Elsheikh B. Cytotoxic Effect of Chitosan Based Nanocomposite Synthesized by Radiation: In Vitro Liver and Breast Cancer Cell Line. J Pharm Pharmacol. 2018;6(4).
34. Souza TGF, Ciminelli VST, Mohallem NDS. A comparison of TEM and DLS methods to characterize size distribution of ceramic nanoparticles. J. Phys. Conf. 2016;733:012039.